Title
Superhydrophobic turbulent drag reduction as a function of surface grating parameters

Authors
Park, H
Sun, G
Kim, CJ

Publication Date
2014-05-25

DOI
10.1017/jfm.2014.151

Authors' final manuscript for: H. Park, G. Sun, and C.-J. Kim, "Superhydrophobic turbulent drag reduction as a function of surface grating parameters," *Journal of Fluid Mechanics*, Vol. 747, May 2014, pp. 722-734. (doi: 10.1017/jfm.2014.151)

Superhydrophobic turbulent drag reduction as a function of surface grating parameters

Hyungmin Park, Guangyi Sun and Chang-Jin "CJ" Kim

Mechanical and Aerospace Engineering Department, University of California at Los Angeles, (UCLA), Los Angeles, CA 90095, USA

Despite the confirmation of slip flows and successful drag reduction in small-scaled laminar flows, the full impact of superhydrophobic (SHPo) drag reduction remained questionable because of the sporadic and inconsistent experimental results in turbulent flows. Here we report a systematic set of bias-free reduction data obtained by measuring the skin-friction drags on a SHPo surface and a smooth surface at the same time and location in a turbulent boundary layer flow. Each monolithic sample consists of a SHPo surface and a smooth surface suspended by flexure springs, all carved out from a 2.7×2.7 mm^2 silicon chip by photolithographic microfabrication. The flow tests allow continuous monitoring of the plastron on the SHPo surfaces, so that the drag reduction data are genuine and consistent. A family of SHPo samples with precise profiles reveals the effects of grating parameters on turbulent drag reduction, which was measured to be as much as ~ 75%.

1. Introduction

Reducing the drag of marine vehicles via gas lubrication has long been practiced by injecting gas bubbles or creating a cavitation gas pocket (Ceccio 2010) and reached a significant drag reduction (~ 95%) at a high Reynolds number ($Re_x \sim 10^7$) flow (Lay *et al*. 2010). Since the gas film (or bubbles) does not stay on the solid surface by nature, however, these methods should continue supplying the gas with additional energy, overshadowing the benefit of drag reduction and limiting applications. The prospect of retaining the gas without energy input has been driving the recent explosive interest in superhydrophobic (SHPo) surfaces – a rough surface of a hydrophobic material. Surface roughness generally increases the skin-friction drag in turbulent boundary layer (TBL) flows (Jimenez 2004) except for very few specific conditions (Walsh 1982). However, if the hydrophobic roughness of the SHPo surface retains microscale air pockets and thus maintains a plastron, the resulting slip flow may bring an appreciable drag reduction. Recent establishment in the slips and drag reductions obtained on engineered SHPo surfaces in laminar flows (Ou *et al*. 2004; Choi & Kim 2006) have heightened the anticipation that someday an appreciable reduction can be reliably obtained in TBL flows as well (Rothstein 2010; Samaha *et al*. 2012b). While most SHPo surfaces in the literature were characterized simply by liquid droplets on them and not

designed to produce any useful amount of slip or drag reduction in continuous liquid flows (Bocquet & Lauga 2011), some studies started identifying and tackling the issues important to engineer drag-reducing SHPo surfaces, such as: how to increase the effective slip (Lee *et al*. 2008; Lee & Kim 2009) and how to maintain the plastron in several adverse conditions representing realistic flows (Lee & Kim 2011, 2012).

Despite an underlying premise for SHPo drag reduction, the state of plastron has not been receiving proper attention in most experimental studies. Its existence has been checked only casually and its detailed state during the flow tests widely ignored. The importance has been recognized only very recently, as the plastron loss became the main roadblock against testing SHPo surfaces in turbulent flows especially in large facilities. Samaha *et al*. (2012a) have measured that the longevity of the plastron was shortened as the flow rate over the SHPo surface increased, and Emami *et al*. (2013) have numerically investigated the unsteady behavior of the plastron interface by considering the diffusion of trapped air over time. They showed that the maximum hydrostatic pressure sustainable above the plastron decreases with increasing width of the water-air interface. Since the loss of plastron is inevitable in practice, Lee & Kim (2011) have developed a semi-active SHPo surface implemented with a self-regulated gas-generation mechanism, which allows indefinite plastrons.

The drag reduction in laminar flows has been well established in recent years, as the slip is predictably related to the SHPo surface parameters (Lauga & Stone 2003; Lee *et al*. 2008). However, such a relationship has yet to be established for turbulent flows (Park *et al*. 2013). While the analytical, numerical and experimental results of SHPo drag reduction converged finally for laminar flows (Lauga & Stone 2003; Ou *et al*. 2004; Choi & Kim 2006; Choi *et al*. 2006; Maynes *et al*. 2007; Woolford *et al*. 2009a), the studies of turbulent flows have mostly been numerical. Assuming ideal circumstances, e.g., no air loss and flat air-water interface, numerical efforts nevertheless have suggested valuable physical insights, such as the possible mechanism of turbulent drag reduction (Min & Kim 2004; Martell *et al*. 2009, 2010; Busse & Sandham 2012; Park *et al*. 2013), scaling issue (Fukagata *et al*. 2006; Jeffs *et al*. 2010; Busse & Sandham 2012; Park *et al*. 2013), and effects of directional slip (Min & Kim 2004; Fukagata *et al*. 2006; Hasegawa *et al*. 2011; Busse & Sandham 2012). For the mechanism of drag reduction, Min & Kim (2004) and Park *et al*. (2013) have reported that surfaces with a streamwise slip lead to weakened near-wall turbulence structures, resulting in skin-friction drag reduction. Martell *et al*. (2010), on the other hand, reported that SHPo surfaces do not affect the nature of near-wall turbulence structures but simply shift them toward SHPo surfaces.

With only a few experimental data in the literature (Henoch *et al*. 2006; Zhao *et al*. 2007; Daniello *et al*. 2009; Woolford *et al*. 2009b; Peguero & Breuer 2009; Jung & Bhushan 2010) scattered by different

flow conditions, surface geometries, and measurement techniques (table 1), the physics of turbulent drag reduction on SHPo surfaces could not be investigated in earnest. To make things worse, these sporadic results have been inconsistent and unsuccessful at suggesting any trend of drag variation with SHPo surface geometry. While some studies (Henoch *et al*. 2006; Daniello *et al*. 2009; Woolford *et al*. 2009b; Jung & Bhushan 2010) reported a substantial drag reduction - up to ~ 18% (~ 50% if both walls of the channel are SHPo) (Daniello *et al*. 2009), others (Zhao *et a*l. 2007; Peguero & Breuer 2009) claimed that the slip on SHPo surfaces has negligible effects in turbulent flows. In our view, possible reasons for the inconsistency include: (i) partial or complete loss of air pockets, i.e., damaged plastron, (ii) a grossly thick air layer formed above the surface, i.e., overgrown plastron, (iii) systematic errors caused by indirect estimation of drag based on velocity profile or pressure drop, and (iv) the effective slip being simply too small to modify the turbulence. Furthermore, most tests were limited to channel flows rather than TBL flows representing the main applications such as marine vessels and underwater structures. With all things considered, it has not been completely clear whether a SHPo surface can generate an appreciable drag reduction in TBL flows. A systematic set of reliable experimental data is sorely missing to confirm and study SHPo drag reduction in turbulent flows.

Challenged by the nagging doubt against the SHPo drag reduction in TBL flows, the present study aims to experimentally confirm the drag-reduction capability of SHPo surfaces in TBL flows beyond any doubt and learn how the SHPo surface geometries affect the reduction. To solve all the above-listed problems that possibly hindered the previous studies and ensure reliable results, we have (i, ii) designed experiments that facilitate an easy and clear monitoring of the plastron state on the sample throughout the flow tests and (iii) devised a method to read the reduction of wall-shear stress directly with little experimental uncertainties (iv) using SHPo surface geometries proven for large slip lengths. By lifting the fundamental doubt and establishing an approach to engineer the SHPo surface, we hope to convince the flow-control community to move on and investigate the hydrodynamics of SHPo surfaces more vigorously toward real-world implementations.

2. Experimental setup

2.1. Device for SHPo drag reduction measurement

To resolve the first two issues raised above, which were commonly overlooked in the literature despite its importance, our experimental setup allows continuous monitoring of the plastron on the SHPo surface throughout the flow tests. To resolve the third issue, we have developed a method to measure the skin-friction drag reduction on a SHPo surface in a direct manner with practically no bias errors. There have been long efforts to develop a robust method to measure the skin-friction drag accurately (Naughton & Sheplak 2002); however, the problem still remained. Our main strategy is to measure the variation of the skin-friction drag directly and comparatively. As illustrated in figure 1(a), which also defines the geometric parameters of the considered SHPo micrograts, a SHPo (i.e., slip) surface and a smooth (i.e., no-slip) surface (as a reference) are placed side-by-side in a sample, each suspended by an identical set of eight micro flexure beams, which directs the two surfaces to displace only in one dimension. All the elements of the 27 × 27 mm^2 sample were carved out from a silicon wafer by photolithographic processes in an integrated-circuit clean room (see supplementary material for details), so the two sets of flexure beams share the same processing conditions and variations during the fabrication. As a result, the two surfaces were floated by the same spring constant. This monolithic sample was flush-mounted on the upper wall of the water-tunnel test section (figure 1b) so that the two surfaces were always under the same flows. This guarantees that any variations in both sample fabrication and flow condition are shared by the two (slip and no-slip) surfaces, so their relative shifting is solely due to the difference in the skin-friction drag acting on them.

Because a suspended surface shifts proportionally to the skin friction on it, the drag on each surface (F_s) is measured directly by reading the displacement (d) of the surface with respect to a built-in ruler (figure 1a) with the relation of $d = (l^3/24EI)F_s$, where l is the length of each flexure beam, E is Young's modulus (169 GPa for silicon), and I is the second moment of area for beam cross section ($I = tw^3/12$, t is the thickness and w is the width). The nominal dimensions of the flexure beams are l = 2500μm, t = 100μm, and w = 15μm. Actual dimensions may be slightly different, w being the parameter affected by the fabrication the most and also affecting the displacement the most. Before running the flow tests, the widths of all the flexure beams were confirmed to be within 5% of the design. Note that, even if the measured drags are not accurate in their absolute values, their relative values are always accurate. The side-by-side configuration of smooth and SHPo surfaces calls for consideration of potential secondary effects. First, the difference in wall-shears and the resulting pressure gradient between the two surfaces may induce a secondary flow between them in spanwise direction. A rough order-of-magnitude comparison between the time-scale for main (streamwise) and induced (spanwise) flows over the sample (see the supplementary materials for details) indicates that the effect of the induced flow, if any, would be very small. Second, the added flow on the SHPo surface by the spanwise inflows may increase the drag

on the SHPo surface, overestimating the SHPo drag (i.e., underestimating DR). The order-of-magnitude analysis further indicates that the increase in the flow speed on the SHPo surface and the resulting drag overestimation are also negligibly small. Even without the comparative reading adopted here, MEMS-based sensor (using a floating element) has shown the most promise to obtain high resolution, instantaneous and fluctuating shear-stress measurements (Naughton & Sheplak 2002). Lastly, the fourth issue has been resolved by fabricating SHPo surfaces of grating patterns with known slip lengths (Lee *et al*. 2008).

2.2. SHPo surface structure

To investigate the effect of surface geometry and explore the maximum drag reduction obtainable under the considered flow condition, we varied the pitch (P) and gas fraction (GF) of the micrograts on SHPo surfaces. Defined as the ratio of the liquid-gas interfacial area to the overall projected area, GF is related to the width (W) and pitch (P) of the grates as $GF = (P - W)/P$ (figure 1a). Two sets of parametric studies were performed by varying P and GF. The first was designed to fix $P = 50\mu m$ and vary $W = 2.5 - 35\mu m$ to achieve $GF = 30 - 95\%$. The second was to fix $P = 100\mu m$ and vary $W = 5 - 50\mu m$ to produce $GF = 50 - 95\%$.

2.3. Water-tunnel setup

A series of flow tests have been performed in a water tunnel, whose test section is 610 mm × 50 mm × 50 mm in the streamwise, vertical, and spanwise directions, respectively), at frictional Reynolds number $Re_\tau = u_\tau \delta / \nu \sim 250$, based on the friction velocity u_τ, boundary-layer thickness δ (both obtained from the boundary-layer profile measured using laser Doppler velocimetry), and kinematic viscosity ν, which roughly corresponds to $Re_x \sim 10^5 - 10^6$ common for a small unmanned underwater vehicle at cruise. The boundary-layer profile of the testing flow followed the "log law" of turbulent flows and showed no effect of adverse pressure gradient, confirming a TBL flow over the current sample location (see figures S5 and S6 in supplementary material). Special efforts were given to verify the flow is of TBL because of the relatively small Reynolds number. To measure the instantaneous displacements of the floating surface in a turbulent flow, a high-speed camera (Vision Research Phantom V7.2) equipped with a light source and an objective lens (×20) was used at 500 fps. The mechanical vibration generated by the pump-pipes system of the water tunnel was first confirmed too small to affect the measurement. After each

measurement, it was confirmed that the floating surfaces return to the initial positions, to make sure there was no permanent effect of the flows on the surfaces. The 50 fps data points (see figure 2) have been reduced from the raw 500 fps images. Recorded displacements were analyzed to obtain the statistical data (time-averaged displacement and rms fluctuation) with ImageJ software. Since the natural frequency of the current floating surface is only about 40 Hz, the fluctuating characteristics of measured displacement (i.e., drag) is originated from the flow condition (i.e., turbulence).

3. Results and discussions

3.1. Turbulent drag reduction on SHPo surfaces

Shown in figure 2 are the pictures of instantaneous displacements captured for three exemplary samples, i.e., three pairs of SHPo and smooth surfaces, along with the temporal variation of displacement measured for each corresponding sample. Depending on the surface geometry, the SHPo surface may show a distinctively smaller displacement (i.e., smaller drag) than the smooth surface, while the difference indicates the drag reduction (DR). As shown in figure 2(a), the SHPo surface of 50μm pitch and 30% *GF*, which would produce a relatively small surface slip (~ 2μm) (Lauga & Stone 2003), displaces (i.e., drags) nearly as much as the smooth surface, indicating little DR. However, the SHPo surfaces of higher GF with larger slips (~ 10 and 33μm) (Lauga & Stone 2003) displace distinctively less than their smooth counterparts (figures 2b and c), clearly indicating a DR. These results provide strong evidence of drag reduction by SHPo surfaces in a TBL flow with a clear trend by their geometric parameters for the first time. Considering many other unsuccessful attempts, the success additionally emphasizes the importance of properly designed and fabricated surface profiles for turbulent drag reduction. Only after microscopic details of the SHPo structures had been refined further from those developed for the laminar flows (Lee et al. 2008; Lee & Kim 2009), was a stable air-water interface guaranteed and a reliable DR obtained in the present TBL flow.

For each sample, the time-averaged displacement of the SHPo surface was normalized to that of the smooth surface in order to produce a normalized SHPo drag rate without a bias error. By collecting the data of all the samples, figure 3(a) reveals how *P* and *GF* of the micrograte affect the SHPo drag reduction in the tested TBL flow. The GF values plotted in figure 3(a) are of the fabricated samples, slightly different from the nominal values of the design. For both 50μm and 100μm pitch, the drag on

SHPo surfaces decreases with *GF*, reaching as small as 25% at *GF* = 0.95. This DR of 75% is significantly larger than the previously largest DR of ~ 18% on a SHPo surface (Daniello et al. 2009). Furthermore, figure 3(a) shows that 100μm pitch reduces the drag more than 50μm pitch does for a given *GF*. The trend of a smaller drag on a larger pitch is somewhat expected from the larger slip confirmed in the laminar flow (Choi et al. 2006; Lee et al. 2008) and the smaller drag found in a turbulent channel flow (Daniello et al. 2009). Interestingly, the effect of pitch is shown to diminish when GF is very large. At *GF* ~ 50%, for example, the DR is more than doubled when the pitch increases from 50μm to 100μm. At *GF* > 90%, however, the DR only slightly increases with the pitch; instead the *GF* plays a bigger role. Currently it is not clear which parameter dominates in determining the drag reduction. Contributions of various parameters will be discussed as a scaling issue in section 3.3.

3.2. Comparison with previous studies

Examining table 1, one may find that some SHPo surfaces with longitudinal grates in micro-scale reported a drag reduction while no SHPo surface with nano-scale grates or random structures produced any positive results. We believe the nano-scale slip lengths on nano-scale grates were too small to be effective in the tested flow systems, and the spanwise slip on random structures negated the drag reduction created by the streamwise slip (Hahn et al. 2002; Min & Kim 2004; Busse & Sandham 2012). Based on this observation, we will compare the present results only with the previous works on micro-scale grates. In figure 3(a), two experimental data (two hollow symbols) from Daniello et al. (2009) and Woolford et al. (2009b) are added for comparison. Since DR was more than doubled when both the upper and lower channel walls were SHPo instead of only one wall (Daniello et al. 2009), indicating the confinement effect of channel flows, the result with one SHPo wall is plotted for a fair comparison. Although they were performed in channel flows, their Reynolds numbers (Re_τ~ 180 and 100, estimated from the data provided (Daniello et al. 2009; Woolford et al. 2009b)) were similar to the current study in a TBL flow (Re_τ~ 250). Considering their pitches and *GF*'s, the 11% (◊ in figure 3a) (Woolford et al. 2009b) and 18% DR (Δ in figure 3a) (Daniello et al. 2009) look reasonable when compared with the current data. Thus, the current trend of DR variation with SHPo surface geometry needs to be tested at different (higher) Reynolds numbers in future studies.

3.3. Scaling

Figure 3(a) indicates that as *GF* increases the drag decreases, ultimately approaching the zero drag. The drag decreases very fast after the *GF* becomes very high (e.g., over 0.9), closely resembling the *GF* vs. the inverse of slip length in laminar flows (Lee *et al*. 2008). The maximum DR achievable in turbulent channel flows has been explained by the effective slip length in wall unit ($\lambda^+ = \lambda u_\tau/\nu$) through numerical simulations (Fukagata et al. 2006; Busse & Sandham 2012; Park et al. 2013). They showed that to obtain a substantial DR, the slip length should be comparable to the viscous sublayer thickness, i.e., $\lambda^+ \sim 5$, and that the DR would saturate if the slip length reaches a very large value, $\lambda^+ = O(10^2)$. Main idea for this scaling is that unlike in laminar flows where the DR is a direct consequence of slip, in turbulent flows both direct (slip) and indirect (suppression of near-wall turbulence structures) effects are likely to contribute to DR (Hahn et al. 2002; Min & Kim 2004; Fukagata et al. 2006; Busse & Sandham 2012; Park et al. 2013). On the other hand, others claimed that the spacing (k) of SHPo surface features (e.g., $k = P - W$ in case of micrograte) is more important than the *GF*, based on their numerical simulations (Martell et al. 2010) and experiment (Daniello et al. 2009) on turbulent channel flows. It was claimed that to impact the turbulent flow, the spacing in wall unit should reach the thickness of the viscous sublayer, i.e., $k^+ \sim 5$, and that as the Reynolds number increases, the DR would approach a limit, which is identical to the *GF* value (Daniello et al. 2009). For the present SHPo surface geometries, the spacing of the micrograte is $k^+ = 0.3 - 2$ in wall unit, which is in a similar range with Daniello et al. (2009). However, the cases of 50μm pitch with 90% and 95% *GF* ($k^+ = 0.91$ and 0.97, respectively) showed much larger DR than the cases of 100μm pitch with 50% and 70% GF ($k^+ = 1$ and 1.4, respectively), indicating that the spacing alone is not a proper parameter to characterize the DR and we need to consider the effects from other parameters as well. Recently, Park et al. (2013) revealed, from a direct numerical simulation on turbulent channel flows with SHPo walls, that the amount of DR for different gratings and Reynolds numbers was well scaled with λ^+, i.e., the skin-friction drag decreased with increasing slip length λ^+. The effect of increasing λ^+ was saturated at $\lambda^+ > 40$, indicating that high skin-friction in wall-bounded turbulent flows are largely attributed to the turbulence structures which are primarily found in the buffer layer ($y^+ = 10-50$) (Kim 2011). With the present data, a clear relationship could not be established between the turbulent DR and the effective slip length λ estimated by the laminar analytical solution (Lauga & Stone 2003), unlike the laminar case where DR could be determined from λ in comparison with the characteristic length (e.g., channel height) (Choi *et al*. 2006). The difference is evident as the drag reduction measured in the present study is much larger than what would be estimated from the laminar analytical solution. This scaling issue is very important to design SHPo surfaces for very high Reynolds number flows and needs to be confirmed experimentally in future studies.

3.4. Comments on the plastron stability

All the present data were obtained with the SHPo surfaces maintaining the plastron as designed; all the air pockets were confirmed to sustain without any loss or merging for hours - much longer than needed to complete testing a sample (~ 30 min). Noting almost no mentioning in the literature on the state of the plastron despite its frailty during the flow tests and suspecting such an oversight is the main reason for the inconsistent results in many SHPo drag reduction studies, we designed the experimental setup to allow easy monitoring of the plastron state with naked eyes. The picture of figure 3(b) shows that the wetting condition of the sample surfaces can be continuously monitored during the flow test. The SHPo surface shows a silvery color due to the different refraction index of the air in the plastron while the smooth surface has a dark color. The sample pictured in figure 3(b) had a SHPo surface with the largest pitch and the highest GF (P = 100μm and GF = 95%). Although a larger pitch or higher GF would reduce the drag even more according to the trend (figure 3a), the plastron on such SHPo surfaces were found to become unstable in the given TBL flow, resulting in the loss of air (i.e., wetting). The plastron on SHPo surfaces was found to be less stable at higher GF's, following a similar trend established and explained for laminar flows (Lee & Kim 2009). However, our current knowledge is not mature enough to pinpoint why the plastron is more susceptible to breakdown in turbulent flows compared with laminar flows, other than suspecting several characteristics of turbulent flows such as pressure fluctuation, large shear and shear-rate at the wall, large skin-friction drag, and intermittency. In comparison, in well-controlled laminar flows (Lee et al. 2008), we were able to maintain a plastron on similar surfaces of larger P and higher GF, up to P = 200μm and GF = 98%. Since maintaining the plastron is more critical for real-world applications, where the static and/or dynamic hydrodynamic conditions are harsher under very high Reynolds numbers ($Re_\tau \sim 10^5$), they may require a relatively small pitch for a more robust plastron. Although only one Reynolds number has been used, the current results support the expectation that the DR can remain substantial even on small pitches at very high Reynolds numbers (Min & Kim 2004; Fukagata et al. 2006; Busse & Sandham 2012; Park et al. 2013). The decreasing DR on the decreasing pitch would be countered by decreasing viscous length scale (i.e., viscous sublayer thickness) of an increasing Reynolds number. While the overall trend is encouraging, more research is needed to quantify the trend and identify limitations.

4. Conclusions

In the present study, we have experimentally confirmed that the SHPo surfaces reduce the skin-friction drag in turbulent flows, assisted by the direct and comparative measurement of skin-friction drag. Within the considered ranges, ~ 75% DR has been achieved and the clear trend of DR as a function of surface grating parameters has been suggested. The present result is exciting because of the significant benefits expected. For instance, in maritime transportation the skin-friction contributes to 60 − 70% of the total drag on a cargo ship and 80% on a tanker (Fukuda et al. 2000). Considering that shipping alone accounts for 8.5% of the global oil supply (Reuters press release, June 24, 2008, Shipping wasting 4.37 million barrels of oil a day) and 3.3% of CO2 emissions (Qi & Song 2012), even a mild DR has a global impact for energy saving and greenhouse effect reduction. With the DR on SHPo surfaces in TBL flows confirmed, one can next perform systematic studies with various SHPo surfaces in a wide range of hydrodynamic flows. As the basic design knowledge is now acquired, time is ripe to focus on more practical issues, such as the longevity (stability) of plastron in the flow conditions of large vessels (e.g., $Re_\tau \sim 10^5$); the development of a low-cost mass production for the SHPo surfaces; and the methodology of deploying SHPo surfaces in real-world applications.

This work has been supported by the ONR Grant (No. N000141110503). The authors thank John Kim and Hyunwook Park for fruitful discussions, MSE Inc. (Pasadena, USA) for providing velocity profiles of turbulent boundary layer flows, and Ryan Freeman for help with the manuscript.

Supplementary materials are available online.

REFERENCES

Bocquet, L. & Lauga, E. 2011 A smooth future? *Nat. Mater*. 10, 334–337.

Busse, A. & Sandham, N. D. 2012 Influence of an anisotropic slip-length boundary condition on turbulent channel flow. *Phys. Fluids* 24, 055111.

Ceccio, S. L. 2010 Friction drag reduction of external flows with bubble and gas injection. *Annu. Rev. Fluid Mech*. 42, 183–203.

Choi, C.-H. & Kim, C.-J. 2006 Large slip of aqueous liquid flow over a nanoengineered superhydrophobic surface. *Phys. Rev. Lett*. 96, 066001.

Choi, C.-H., Ulmanella, U., Kim, J., Ho, C.-M. & Kim, C.-J. 2006 Effective slip and friction reduction in nanograted superhydrophobic microchannels. *Phys. Fluids* 18, 087105.

Daniello, R. J., Waterhouse, N. E. & Rothstein, J. P. 2009 Drag reduction in turbulent flows over superhydrophobic surfaces. *Phys. Fluids* 21, 085103.

Emami, B., Hemeda, A. A., Amrei, M. M., Luzar, A., Gad-el-Hak, M. & Tafreshi, H. V. 2013 Predicting longevity of submerged superhydrophobic surfaces with parallel grooves. *Phys. Fluids* 25, 062108.

Fukagata, K., Kasagi, N. & Koumoutsakos, P. 2006 A theoretical prediction of friction drag reduction in turbulent flow by superhydrophobic surfaces. *Phys. Fluids* 18, 051703.

Fukuda, K., Tokunaga, J., Nobunaga, T., Nakatani, T., Iwasaki, T. & Kunitake, Y. 2000 Frictional drag reduction with air lubricant over a super-water-repellent surface. *J. Mar. Sci. Techno*. 5, 123–130.

Hahn, S., Je, J. & Choi, H. 2002 Direct numerical simulation of turbulent channel flow with permeable walls. *J. Fluid Mech*. 450, 259–285.

Hasegawa, Y., Frohnapfel, B., & Kasagi, N. 2011 Effects of spatially varying slip length on friction drag reduction in wall turbulence. *J. Phys.: Conf. Ser*. 318, 022028.

Henoch, C., Krupenkin, T. N., Kolodner, P., Taylor, J. A., Hodes, M. S., Lyons, A. M., Peguero, C. & Breuer, K. 2006 Turbulent drag reduction using superhydrophobic surfaces. AIAA Paper 2006-3192.

Jeffs, K., Maynes, D. & Webb, B. W. 2010 Prediction of turbulent channel flow with superhydrophobic walls consisting of micro-ribs and cavities oriented parallel to the flow direction. *Int. J. Heat Mass Tran*. 53, 786–796.

Jimenez, J. 2004 Turbulent flows over rough walls. *Annu. Rev. Fluid Mech*. 36, 173–196.

Jung, Y. C. & Bhushan, B. 2010 Biomimetic structures for fluid drag reduction in laminar and turbulent flows. *J. Phys.: Condens. Matter* 22, 035104.

Kim, J. 2011 Physics and control of wall turbulence for drag reduction. *Phil. Trans. R. Soc. A* 369, 1396–1411.

Lauga, E. & Stone, H. 2003 Effective slip in pressure-driven stokes flow. *J. Fluid Mech*. 489, 55–77.

Lay, K. A., Ryo, Y., Simo, M., Perlin, M. & Ceccio, S. L. 2010 Partial cavity drag reduction at high Reynolds numbers. *J. Ship Res*. 54, 109–119.

Lee, C., Choi, C.-H. & Kim, C.-J. 2008 Structured surfaces for a giant liquid slip. *Phys. Rev. Lett*. 101, 064510.

Lee, C. & Kim, C.-J. 2009 Maximizing the giant liquid slip on superhydrophobic microstructures by nanostructuring their sidewalls. *Langmuir* 25, 12812–12818.

Lee, C. & Kim, C.-J. 2011 Underwater restoration and retention of gases on superhydrophobic surfaces for drag reduction. *Phys. Rev. Lett*. 106, 014502.

Lee, C. & Kim, C.-J. 2012 Wetting and active dewetting processes of hierarchically constructed superhydrophobic surfaces fully immersed in water. *J. Microelectromech S*. 21, 712–720.

Martell, M. B., Perot, J. B. & Rothstein, J. P. 2009 Direct numerical simulations of turbulent flows over superhydrophobic surfaces. *J. Fluid Mech*. 620, 31–41.

Martell, M. B., Rothstein, J. P. & Perot, J. B. 2010 An analysis of superhydrophobic turbulent drag reduction mechanisms using direct numerical simulation. *Phys. Fluids* 22, 065102.

Maynes, D., Jeffs, K., Woolford, B. & Webb, B. W. 2007 Laminar flow in a microchannel with hydrophobic surface patterned microribs oriented parallel to the flow direction. *Phys. Fluids* 19, 093603.

Min, T. & Kim, J. 2004 Effects of hydrophobic surface on skin-friction drag. *Phys. Fluids* 16, L55–L58.

Naughton, J. W. & Sheplak, M. 2002 Modern developments in shear-stress measurement. *Prog. Aero. Sci*. 38, 515–570.

Ou, J., Perot, B. & Rothstein, J. P. 2004 Laminar drag reduction in microchannels using ultrahydrophobic surfaces. *Phys. Fluids* 16, 4635–4643.

Park, H., Park, H. & Kim, J. 2013 A numerical study of the effects of superhydrophobic surface on skin-friction drag in turbulent channel flow. *Phys. Fluids* 25, 110815.

Peguero, C. & Breuer, K. 2009 On drag reduction in turbulent channel flow over superhydrophobic surfaces. In *Advances in Turbulence XII* (ed. B. Eckhardt), pp. 233–236. Springer-Verlag.

Qi, X. & Song, D.-P. 2012 Minimizing fuel emissions by optimizing vessel schedules in liner shipping with uncertain port times. *Transp. Res. Part E* 48, 863–880.

Rothstein, J. P. 2010 Slip on superhydrophobic surfaces. *Annu. Rev. Fluid Mech*. 42, 89–109.

Samaha, M. A., Tafreshi, H. V. & Gad-el-Hak, M. 2012a Influence of flow on longevity of superhydrophobic coatings. *Langmuir* 28, 9759–9766.

Samaha, M. A., Tafreshi, H. V. & Gad-el-Hak, M. 2012b Superhydrophobic surfaces: from the lotus leaf to the submarine. *C.R. Mec*. 340, 18–34.

Walsh, M. J. 1982 Turbulent boundary layer drag reduction using riblets. AIAA Paper 1982-0169.

Woolford, B., Maynes, D. & Webb, B. W. 2009a Liquid flow through microchannels with grooved walls under wetting and superhydrophobic conditions. *Microfluid. Nanofluid*. 7, 121–135.

Woolford, B., Prince, J., Maynes, D. & Webb, B. W. 2009b Particle image velocimetry characterization of turbulent channel flow with rib patterned superhydrophobic walls. *Phys. Fluids* 21, 085106.

Zhao, J., Du, X. & Shi, X. 2007 Experimental research on friction-reduction with superhydrophobic surfaces. *J. Mar. Sci. Appl*. 6, 58–61.

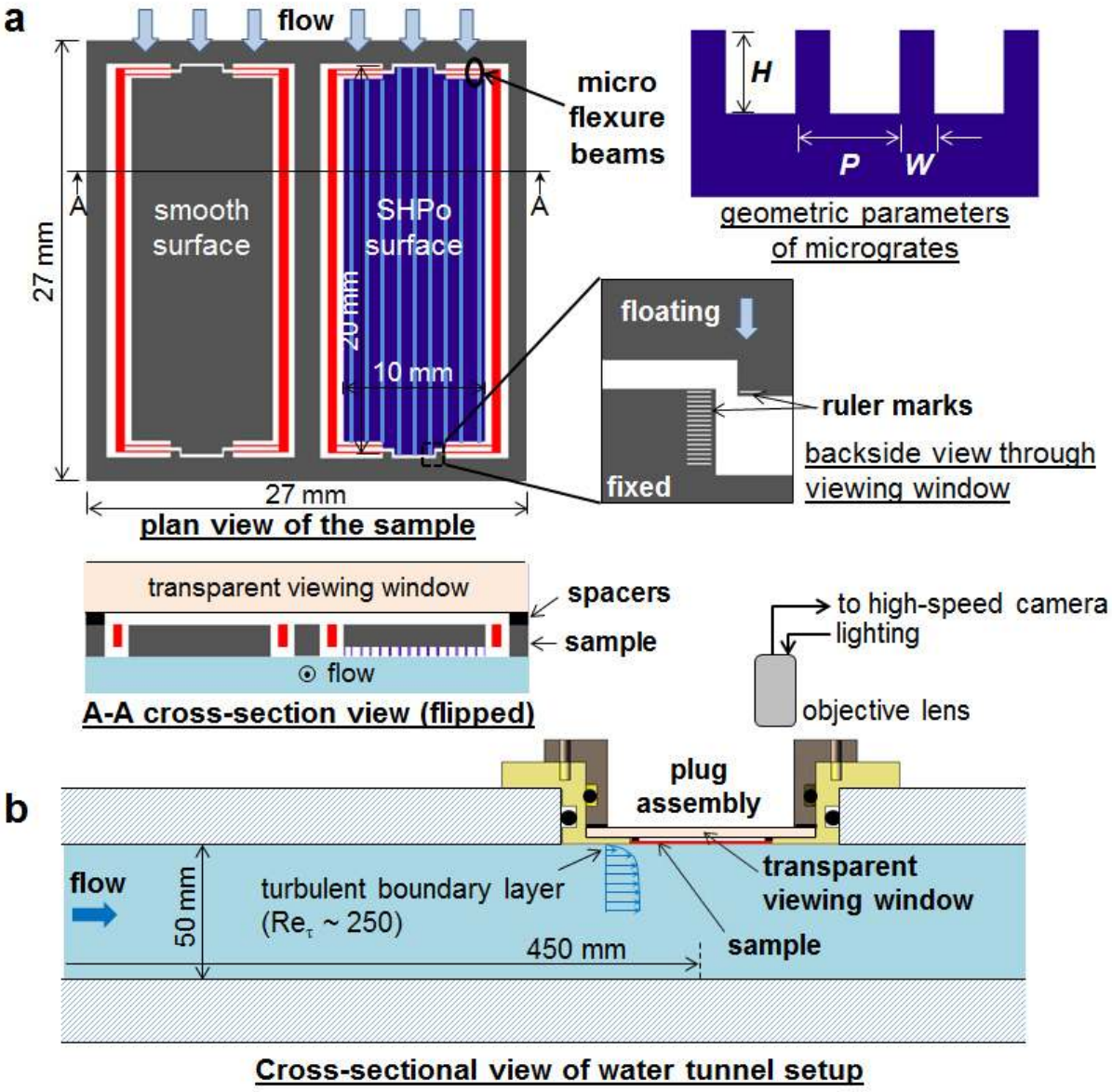
a
flow
micro flexure beams
H
P
W
geometric parameters of microgrates
smooth surface
SHPo surface
A
A
27 mm
20 mm
10 mm
27 mm
plan view of the sample
floating
ruler marks
backside view through viewing window
fixed
transparent viewing window
spacers
sample
flow
A-A cross-section view (flipped)
to high-speed camera
lighting
objective lens
b
plug assembly
flow
50 mm
turbulent boundary layer
(Re$_\tau$ ~ 250)
transparent viewing window
450 mm
sample
Cross-sectional view of water tunnel setup

Authors' final manuscript for: H. Park, G. Sun, and C.-J. Kim, "Superhydrophobic turbulent drag reduction as a function of surface grating parameters," *Journal of Fluid Mechanics*, Vol. 747, May 2014, pp. 722-734. (doi: 10.1017/jfm.2014.151)

Figure 1. Schematic figures of (a) a sample consisting of a SHPo and a smooth surface each suspended by an identical set of flexure beam springs and (b) water tunnel setup with the sample flush-mounted on the top inside wall (drawn not to scale).

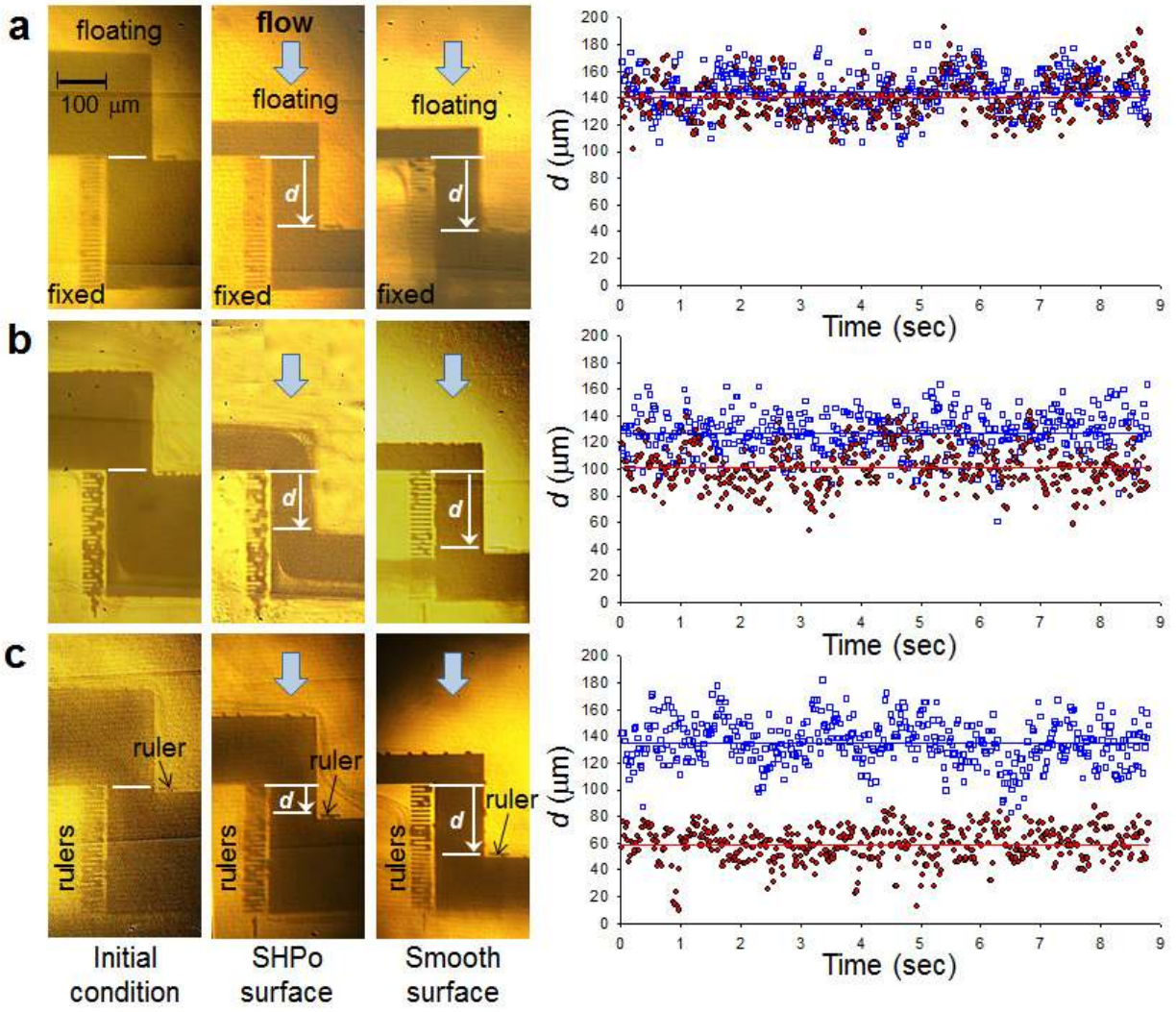

Figure 2. Instantaneous images of SHPo (second column) and smooth (third column) surfaces captured during flow tests for three different samples: (a) (*P*, *GF*) = (50 μm, 30%); (b) (50 μm, 60%); (c) (50 μm, 90%). Compared with the initial position (first column), the floating surfaces displace along the flow direction (see the arrows) when TBL flows over the sample. The temporal displacements of the SHPo (□) and smooth (□) surfaces are shown in the corresponding graphs (fourth column). Note that the current measurement method captures the fluctuating nature of the turbulent skin-friction drag. The solid lines denote the time-averaged displacements of the floating surfaces.

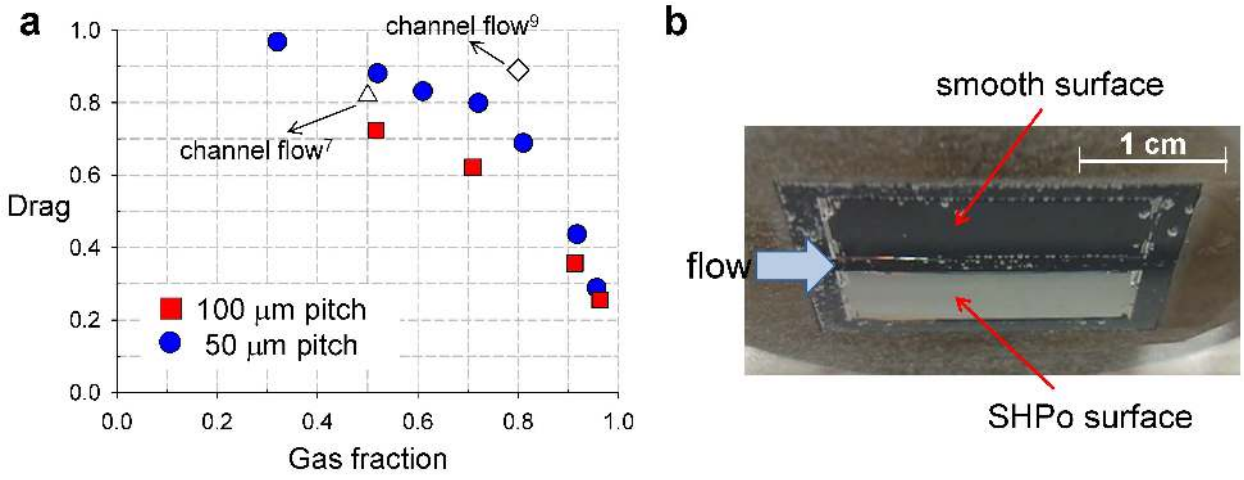

Figure 3. Effect of SHPo surface geometry in TBL flow ($Re_\tau \sim 250$). (a) Variation of normalized drag with gas fraction (*GF*) for pitches of 50 μm (●) and 100 μm (■). Two available results of micrograte SHPo surfaces, although measured in turbulent channel flows, are included for comparison: △, 60 μm pitch and 50% *GF* ($Re_\tau \sim 180$)[7]; ◇, 40 μm pitch and 80% *GF* ($Re_\tau \sim 100$)[9]. (b) Picture of a sample during flow test. Loss of any air pockets (even one trench) or appearance of any rogue bubbles (e.g., merging of neighboring air pockets) was readily detectable; if so (rare), the test was aborted. The SHPo surface in this sample produced the largest reduction rate (~75%) in the current study.